*13th Australasian Fluid Mechanics Conference*
*Monash University, Melbourne, Australia*
*13-18 December 1998*

# THE EFFECT OF LONGITUDINAL MICRO-STRIATIONS AND THEIR PROFILES ON THE DRAG OF FLAT PLATES

**Kamalluddien PARKER[1] and Anthony T. SAYERS[2]**

## ABSTRACT

The use of surface modifications as a means of reducing viscous drag on a body has potential aerodynamic and hydrodynamic applications. V-grooves of specific dimensions are machined in a longitudinal direction, onto the surface of a smooth plate and the resulting effect on the drag force of the plate is observed. Previously conducted experiments have indicated that v-grooves (riblets) could reduce turbulent skin friction drag by up to 7 percent depending on the size and shape of the grooves. The drag reducing performance of riblets with aspect ratios (*h/s*) of 0.22 and 1 respectively, are examined. A boundary layer analysis of the turbulent flow characteristics over the smooth surface and the riblet surfaces indicated an increase in the laminar sublayer thickness and local Reynolds number while reducing the boundary layer thickness for the ribbed surfaces. A maximum drag reduction of 6.83% was recorded for the surface covered with the symmetric riblet, at a Reynolds number of 117101. It is felt that riblets hamper the momentum and turbulent energy exchange from regions of high velocity to lower velocity regions by impeding the cross flow of streamwise vortices that prevail in the viscous sublayer of a turbulent boundary layer. By suppressing these streamwise vortices, turbulent mixing and hence turbulent shear stress is reduced. The results obtained support those of other workers where available.

**Keywords:** turbulent, boundary, layer, streamwise vortices, riblets, drag, reduction, shear stress.

## INTRODUCTION

The importance of energy conservation has been a driving force behind the initiation of research into methods that will reduce the turbulent skin friction drag on transport aircraft fuselages. Fuselage skin-friction reductions as small as 10 percent provide the potential for a 500 million dollar per year fuel saving for the airlines. In the past several years significant efforts have been made to develop passive techniques which effect a net reduction in surface shear stress due to boundary layer turbulence. One technique that has demonstrated net surface drag reduction and has the potential for practical aerodynamic and hydrodynamic applications is the use of streamwise triangular v-groove or riblet surface modifications. Surface modifications seem to be the most attractive of the passive devices investigated so far, simply because they require little or no maintenance and are relatively easy to install.

Walsh [1-3] showed that a surface with a v-shape geometry for the grooves could give surface drag reductions of up to 8 percent. Other shapes of grooves that have been studied [4-8] include rectangular and rounded v-grooves, while upstream flow histories were varied [9,10] to see the effects of changing free stream Reynolds numbers and turbulent intensities when grooves were present. Experiments on aerofoil surfaces [11,12] indicate that boundary layer separation was delayed in adverse pressure gradients when the surfaces of the aerofoils were grooved. Visualisation of the flow in the grooves has been attempted using dye and hydrogen bubble flow techniques [13], large scale models [14] and three dimensional particle velocimetry [15].

The present study combines a turbulent boundary layer analysis with a direct drag measurement analysis. The drag reducing effect of two different v-groove geometry riblets machined on the surface of a smooth flat plate is investigated, since this geometry has shown the greatest potential for drag reduction and is the easiest to manufacture. One ribbed surface is machined with an unsymmetrical v-groove with the rib height-to-rib spacing ratio, *h/s* of 0.22. A second surface is machined with a symmetric v-groove of $h/s = 1$. A smooth plate of the same area is used as the reference plate for the analysis. For direct drag measurements, the plates are suspended at zero angle of attack in a wind tunnel, the flow over the surfaces being turbulent. The boundary layers of the three test surfaces are compared in terms of the shear stress, skin friction coefficient, boundary layer thickness and laminar sublayer thicknesses for each plate.

## NOTATION

$b$ test plate width (m)
$C_D$ dimensionless drag coefficient $\{=D/(0.5\rho u_\infty^2 S)\}$
$C_f$ dimensionless local skin friction coefficient
$D$ total drag force (N)
$h$ riblet height (m)
$h^+$ dimensionless riblet height in law of the wall co-ordinates $\{=(hu_\infty/\nu)\sqrt{C_f/2}\}$
$l$ test plate length (m)
$Re_x$ Reynolds number at distance $x$ from the plate leading edge $(= u_x x/\nu)$
$Re_l$ Reynolds number based on total length of test plate $(= u_\infty l/\nu)$
$s$ riblet spacing (m)
$s^+$ dimensionless riblet spacing in law of the wall co-ordinates $\{=(su_\infty/\nu)\sqrt{C_f/2}\}$
$S$ span area $(= bl)$ $(m^2)$
$u_\infty$ freestream velocity (m/s)
$u^+$ dimensionless shear velocity $\left(= \frac{v_x}{\sqrt{\tau_w/\rho}}\right)$
$v_x$ velocity at a height $y$ above the plate at distance x from the leading edge (m/s)
$x$ distance along plate from leading edge (m)
$y$ vertical distance above test plate surface (m)

1. Mechanical Engineer, Airmotive Division, Denel Aviation, Kempton Park, 1500, SOUTH AFRICA
2. Department of Mechanical Engineering, University of Cape Town, Rondebosch, 7701, SOUTH AFRICA

$y^+$ dimensionless shear height ($= \frac{y\sqrt{\tau_w/\rho}}{\nu}$)

$z$ transverse distance across plate (m)

**Greek**

$\delta$ boundary layer thickness (m)

$\delta_L$ laminar sublayer thickness (m)

$\mu$ dynamic viscosity (Pa s)

$\nu$ kinematic viscosity ($m^2/s$)

$\rho$ fluid density ($kg/m^3$)

$\tau_w$ shear stress at the plate surface (wall) (Pa)

## THEORY

In the absence of an exact solution to describe the behaviour of turbulent boundary layer flow over a flat plate, experimental results are used. The Prandtl one-seventh-root velocity profile correlates well with turbulent boundary layer data over a wide range of Reynolds numbers [16],

$$\frac{v_x}{u_\infty} = \left(\frac{y}{\delta}\right)^{1/7} \quad (1)$$

The wall shear stress is obtained from turbulent pipe flow experimental results [17] in the range $Re_x < 10^7$.

$$\tau_w = 0.029\rho {u_\infty}^2 \left(\frac{\nu}{u_\infty x}\right)^{1/5} \quad (2)$$

The local skin friction coefficient is given by,

$$C_f = \frac{\tau_w}{\frac{1}{2}\rho {u_\infty}^2} \quad (3)$$

The total drag force on the plate is determined by integrating the wall shear stress over the surface area of the plate of length $l$ [16] so that,

$$D = b\int_0^l \tau_w dx = \frac{0.0358\rho {u_\infty}^2 bl}{(\mathrm{Re}_l)^{1/5}} \quad (4)$$

The corresponding coefficient of drag is then [16],

$$C_D = \frac{0.074}{(\mathrm{Re}_l)^{1/5}} \quad (5)$$

and the boundary layer thickness $\delta$, at distance $x$ from the plate leading edge, is calculated from [16],

$$\delta = \frac{0.368x}{(\mathrm{Re}_x)^{1/5}} \quad (6)$$

The thickness of the viscous laminar sublayer is [16],

$$\delta_L = \frac{8\nu}{\sqrt{\tau_w/\rho}} \quad (7)$$

The shear stress at the plate surface at distance $x$ from the leading edge is obtained from the velocity profile through the laminar sublayer and is determined from [16],

$$\tau_w = \mu\left(\frac{dv_x}{dy}\right)_{y=0} \quad (8)$$

Choosing a test plate with dimensions of 300 mm by 520 mm and an air free stream velocity of 3 m/s, the theoretical boundary layer characteristics of a flat plate in turbulent flow were determined at $x$ = 110, 200, 300, 380, 490 and 590 mm from the leading edge of the plate. These results are tabulated in Table 1.

The corresponding boundary layer thickness and laminar sublayer thickness values are shown in Table 2. The total drag force on the smooth plate calculated from equation (4) is 0.008 N. Using equation (5) the corresponding drag coefficient, for the smooth plate was calculated to be 0.00715.

## EXPERIMENTAL METHOD

Two types of experiment were performed. i) Direct boundary layer velocity profile and thickness measurements were made on stationary flat plates, and from the results, the friction coefficients at various points along the plates were determined. ii) The plates were freely suspended from a drag balance such that the drag force caused by the air flow over one surface was measured directly.

### Stationary plate tests

Three test plates were constructed from 10 mm thick perspex sheet. One of the plates was left un-machined with its original smooth surface while one surface of each of the other two plates was machined with v-groves as detailed in figure 1. The wind tunnel in which these plates were placed had a closed jet test section 526 mm square and 880 mm long. Each plate was 720 mm long and horizontally spanned the test section from wall to wall at a height of 210 mm as shown in figure 2. A miniature pitot tube probe was formed from a hypodermic bent through 90 degrees near its tip. The tip was deformed from the round into an oval shape 0.58 mm high by 0.98 mm wide and was suspended above the plate in a three dimensional traverse. A turbulent boundary layer over the whole length of the plate was assured by gluing 40 grit course sandpaper to the elliptical leading edge of each plate. Boundary layer velocity profiles were then measured at a free stream velocity of 3.6 m/s by traversing the pitot probe vertically from the plate surface in increments of 0.1 mm at selected distances $x$ from the plate leading edge.

### Freely suspended plate tests

Direct drag measurements were performed in a re-circulating open jet wind tunnel test section measuring 870 mm x 580mm with corner fillets and a working length of 1.6 m. Each plate was suspended from four 1mm thick spring steel hacksaw blades, the upper ends of which were fixed encastre into a fixed support frame (figure 3). The test surface of the plate was aligned flush with the roof of the tunnel throat where the air stream exited into the test section, such that the airflow over the plate was restricted to the underside surface being tested. Strain gauges mounted on each steel blade near the upper encastre point were calibrated for drag force against a given strain when deflected. The drag on each plate was then measured at free steam velocities in the range 1 to 12 m/s and repeated with the plates turned through 180 degrees. With careful alignment of the plates with the tunnel roof, the individual drag measurements were repeatable to within 5 percent.

## RESULTS

Typical velocity profiles for the three stationary plates are shown in figure 4 at a position 100 mm from the leading edge of the plates. Using selected points within the laminar sublayer region, the velocity gradient at the plate surface at each position along the plate was determined using linear correlation, and hence the wall shear stress at the plate surface calculated from equation (8). Values of $u^+$ and $y^+$ were also calculated and typical data sets are compared with the universal law of the wall curve in figures 5 and 6. Tables 3 to 5 show the boundary layer parameters for each plate calculated from the experimental velocity profiles, while Table 6 compares the boundary layer thickness and laminar sublayer thickness for each of the three experimental plates. Figure 7 shows the variation in local skin friction coefficient along the plate as determined in Tables 3 to 5. Figure 8 shows the drag coefficient $\{D/(0.5\rho u_\infty{}^2 S)\}$ calculated from the direct drag measurements plotted as a function of Reynolds number based on the total length of the plate.

## DISCUSSION

It was important that a truly turbulent boundary layer was achieved over the whole length of the plates and this was assured by comparing the velocity profiles at different locations along the plates with the Prandtl one seventh power law of equation (1) for regions outside the laminar sublayer. The data in figure 4 shows that good correlation with the one seventh power law was achieved, the thickness of the boundary layer being defined at the height above the plate where $v_x = 0.99u_\infty$. Further confirmation that a valid fully turbulent boundary layer was present, was through a comparison of the data with the universal law of the wall curve. Figures 5 to 7 indicate that while the data correlates for regions outside the laminar sublayer, within the laminar sublayer the gradient of the velocity profile is significantly different and therefore a different wall shear stress will arise. Thus, whereas almost all the smooth plate data of figure 5 lies outside the laminar sublayer, that of figures 6, for ribbed plate 1, shows data to be falling well within the laminar sublayer. This is supported by Walsh [7] who comments that unless measurements are made close to the wall, the effects of riblets on the velocity profile will appear to be small or even negligible.

In Tables 1 and 3 the mean difference between the theoretical and experimental shear stresses respectively for the smooth plate is only 0.61%. Similarly, the boundary layer thicknesses for the smooth plate in Tables 2 and 6 show excellent agreement. It is thus concluded that the experimental technique used was sound, and the same analysis was valid for the ribbed plates. In Table 6, the ribbed plates' boundary layers are thinner than for the smooth plate, being on average 1.62% less for plate 1 (large riblets) and 3.03 % less for plate 2, (small riblets). Also, the laminar sublayer thickness is greater for the ribbed plates than the smooth plate. This ultimately indicates a reduction in the momentum exchange between regions of low velocity and high velocity fluid. A reduction in the net exchange of momentum and energy results in a reduction of the force created in the direction of flow, that is a reduction in the wall shear stress. This is evidenced by the reduced values of friction coefficient for the ribbed plates in Tables 4 and 5, compared to the values for the smooth plate in Table 3, and which were calculated from the laminar sublayer velocity gradients. The previous deductions are reinforced in figure (8) by a definite reduction in $C_D$ for the two ribbed plates, with the riblet plate 2 showing the greatest reduction. On average, riblet plate 1 displayed a 3.96% reduction in drag over the smooth plate, while that for riblet plate 2 was 11.59%. However, while the smooth plate $C_D$, which was calculated from the velocity profiles, compared well with theoretical predictions using equation (5), the experimental total drag showed a difference of 17%. The drags for the ribbed plates calculated from the directly measured velocity profiles differed by a maximum of about 7%.

## CONCLUSIONS

Previous riblet research reveals two points of contention on the effect of riblets. It is uncertain whether the effects of riblets on the turbulent structure are primary or secondary. There is however a consensus that the riblets induce a secondary vortex system within the groove valleys and that these vortices provide lateral resistance to the turbulent streamwise vortices, thereby reducing the skin friction component. V-groove riblets can be used as a surface modification in order to reduce the drag on a smooth flat plate.

The theoretical and experimental analysis on the smooth plate compared favourably. A standard deviation of 1.99% was calculated for the two values of friction coefficient for the ribbed plates. The symmetric v-groove riblets with $h/s$ = 1 show the greatest potential, with a drag reduction of 6.83% at a Reynolds number of 117101. The unsymmetrical v-groove riblets with $h/s$ = 0.22 also show a drag reduction potential but to a lesser degree. A drag reduction of 3.73% was recorded at a Reynolds number of 117101. It is apparent that the drag reducing ability of riblets is dependent on the $h/s$ ratio and the Reynolds number regime in which the flow exists. The effects of the v-grooves is to modify and effectively reduce the momentum and energy exchange properties caused by the stream-wise vortices developing near the surface beneath the turbulent layer, with a consequent reduction in shear stress levels. Riblet surfaces are characterised by a decrease in the boundary layer thickness and an increase in the laminar sublayer thickness. This coincides with an increase in the flow Reynolds number.

## REFERENCES


1. Walsh M.J., "Drag Characteristics of v-groove and transverse curvature riblets", *AIAA Journal: Progress in Aeronautics and Astronautics*, **72**, 168-184, 1980.
2. Walsh, M.J., "Turbulent boundary layer drag reduction using riblets", *AIAA Paper 82-0169*, January 1982.
3. Walsh, M.J. and Lindermann, A.M., "Optimization and application of riblets for turbulent drag reduction", *AIAA Paper 84-0347*, March 1984.
4. Lui, C.K., Kline, S.J. and Johnstone, J.P., "Experimental study of a turbulent boundary layer on rough walls", *Report MD-15*, Dept. of Mechanical Engineering, Stanford University, 1966.
5. Kennedy, J.F., Hsu, S.T. and Lin, J.T., "Turbulent flow past boundaries with small streamwise fins", *Journal of the Hydraulics Division, Proceedings of*

*the American Society of Civil Engineers*, **99**, 76-86, April 1973.
6. Walsh, M.J. and Weinstein, L.M., "Drag and heat transfer on surfaces with small longitudinal fins", *AIAA Paper 78-1161*, July 1978.
7. Walsh, M.J., "Riblets as a viscous drag reduction technique", *AIAA Journal*, **21**(4), 485-486, April 1983.
8. Walsh, M.J., "Riblets: viscous drag reduction in boundary layers", *NASA Technical Report*, 203-261, Virginia, 1990.
9. Balint, J.L. and Wallace, J.M., "Viscous drag reductions using streamwise aligned riblets: Survey and new results", Paper presented at IUTAM Symposium, Bangalore, India, January 1987.
10. Gallagher, J.A. and Thomas, A.S.W., "Turbulent boundary layer characteristics over streamwise grooves", *AIAA Paper 84-2185*, 1-8, November 1985.
11. Viswanath, P.R. and Mukund, R., "Turbulent drag reduction using riblets on a supercritical airfoil at transonic speeds", *AIAA Journal*, **33**(5), 945-947, May 1995.
12. Nieuwstadt, F.T.M., Wolther, W., Leijdens, H., Prasad, H.K. and Schwarz-van Manen, A., "The reduction of skin friction by riblets under the influence of an adverse pressure gradient", *Experiments in Fluids*, **15**(1), 17-26, 1993.
13. Bacher, E. and Smith, C.R., "A combined visualisation-anemometry study of triangular micro-grooved surface modifications", *AIAAA Paper 85-0548*, May 1985.
14. Park, S.R. and Wallace, J.M., "Flow alteration and drag reduction by riblets in a turbulent boundary layer", *AIAA Journal*, **32**(1), 31-38, January 1994.
15. Suzuki, Y. and Kasagi, N., "Turbulent drag reduction mechanism over a riblet surface", *AIAA Journal*, **32**(9), 1781-1790, September 1994.
16. Janna, W.S., *Introduction to Fluid Mechanics*, 3rd ed., PWS Publishing, Boston, 1994.
17. Holman, J.P., *Heat Transfer*, 7th ed., McGraw-Hill, New York, 1992.

| $x$ (mm) | $\tau$ (Pa) | $C_f$ | $Re$ |
|---|---|---|---|
| 110 | 0.0607 | 0.007712 | 26661 |
| 200 | 0.0538 | 0.006843 | 48475 |
| 300 | 0.0496 | 0.006310 | 72712 |
| 380 | 0.0473 | 0.006018 | 92102 |
| 490 | 0.0450 | 0.005720 | 118764 |
| 590 | 0.0434 | 0.005511 | 143001 |

**Table 1**: Theoretical boundary layer characteristics for the smooth plate.

| $x$ (mm) | $\delta$ (mm) | $\delta_L$ (mm) |
|---|---|---|
| 110 | 5.27 | 0.53 |
| 200 | 8.51 | 0.56 |
| 300 | 11.77 | 0.59 |
| 380 | 14.22 | 0.60 |
| 490 | 17.42 | 0.62 |
| 590 | 20.21 | 0.63 |

**Table 2**: Theoretical boundary layer and laminar sublayer thickness for the smooth plate.

| $x$ (mm) | $\tau$ (Pa) | $C_f$ | $Re$ |
|---|---|---|---|
| 110 | 0.06182 | 0.00786 | 25991 |
| 200 | 0.05440 | 0.00692 | 88035 |
| 300 | 0.05097 | 0.00648 | 76422 |
| 380 | 0.04609 | 0.00586 | 74050 |
| 490 | 0.04464 | 0.00567 | 121261 |
| 590 | 0.04404 | 0.00560 | 141701 |

**Table 3**: Experimental boundary layer characteristics for the smooth plate.

| $x$ (mm) | $\tau$ (Pa) | $C_f$ | $Re$ |
|---|---|---|---|
| 110 | 0.05670 | 0.00721 | 28045 |
| 200 | 0.05200 | 0.00661 | 91009 |
| 300 | 0.04963 | 0.00631 | 85177 |
| 380 | 0.04342 | 0.00552 | 80611 |
| 490 | 0.04171 | 0.00530 | 134269 |
| 590 | 0.03870 | 0.00492 | 154609 |

**Table 4**: Experimental boundary layer characteristics for riblet surface 1.

| $x$ (mm) | $\tau$ (Pa) | $C_f$ | $Re$ |
|---|---|---|---|
| 110 | 0.05502 | 0.00699 | 31503 |
| 200 | 0.04985 | 0.00634 | 97326 |
| 300 | 0.04899 | 0.00623 | 91009 |
| 380 | 0.04139 | 0.00526 | 84882 |
| 490 | 0.03995 | 0.00508 | 146770 |
| 590 | 0.03733 | 0.00475 | 160570 |

**Table 5**: Experimental boundary layer characteristics for riblet surface 2.

| | Smooth plate | | Riblet plate 1 | | Riblet plate 2 | |
|---|---|---|---|---|---|---|
| $x$ (mm) | $\delta$ (mm) | $\delta_L$ (mm) | $\delta$ (mm) | $\delta_L$ (mm) | $\delta$ (mm) | $\delta_L$ (mm) |
| 110 | 5.30 | 0.527 | 5.22 | 0.550 | 5.100 | 0.558 |
| 200 | 7.55 | 0.561 | 7.50 | 0.574 | 7.400 | 0.586 |
| 300 | 11.65 | 0.580 | 11.40 | 0.588 | 11.250 | 0.592 |
| 380 | 14.85 | 0.610 | 14.60 | 0.628 | 14.450 | 0.643 |
| 490 | 17.35 | 0.620 | 17.00 | 0.641 | 16.700 | 0.655 |
| 590 | 20.25 | 0.624 | 19.90 | 0.665 | 19.750 | 0.678 |

**Table 6**: Experimental boundary layer and laminar sublayer thickness for each plate.

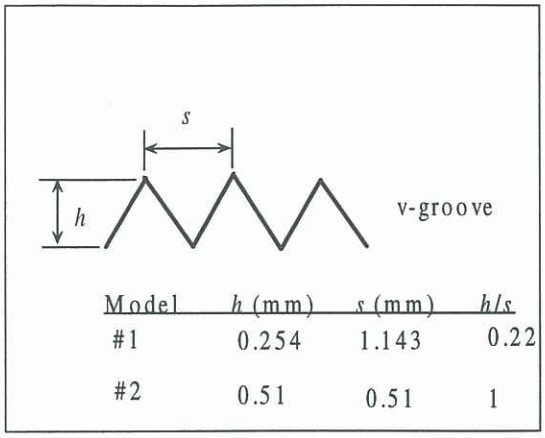


| Model | h (mm) | s (mm) | h/s |
|---|---|---|---|
| #1 | 0.254 | 1.143 | 0.22 |
| #2 | 0.51 | 0.51 | 1 |

**Figure 1**: V-groove riblets.

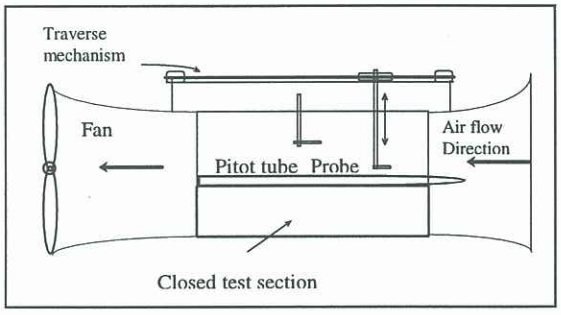


**Figure 2**: Experimental setup for boundary layer measurements

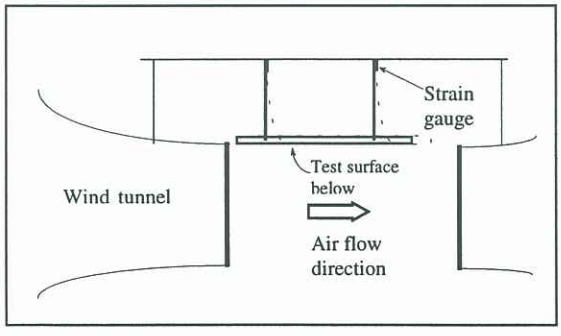


**Figure 3**: Experimental setup for direct drag measurments.

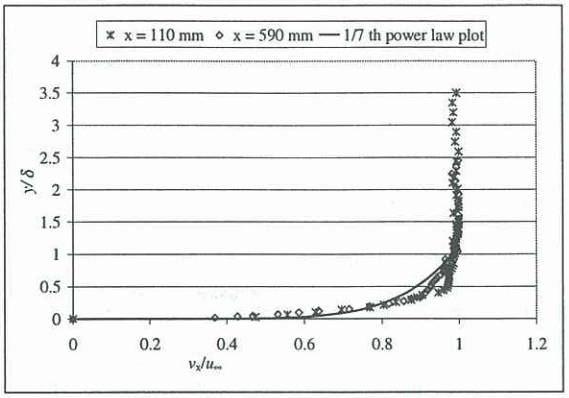


**Figure 4:** Turbulent boundary layer velocity profiles.

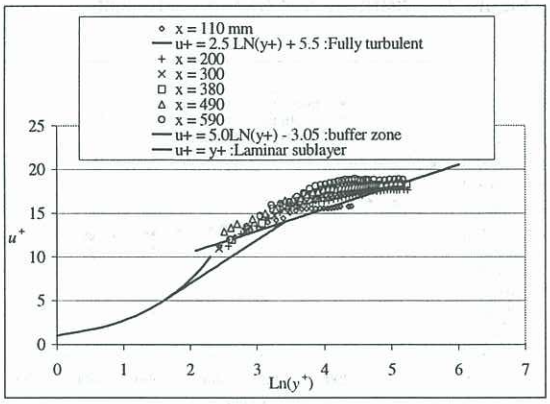


**Figure 5**: Velocity profiles in Law of the Wall co-ordinates for the smooth plate.

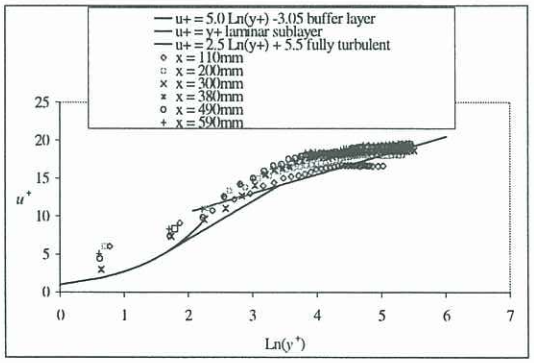


**Figure 6:** Velocity profiles in Law of the Wall co-ordinates for ribbed plate 1.

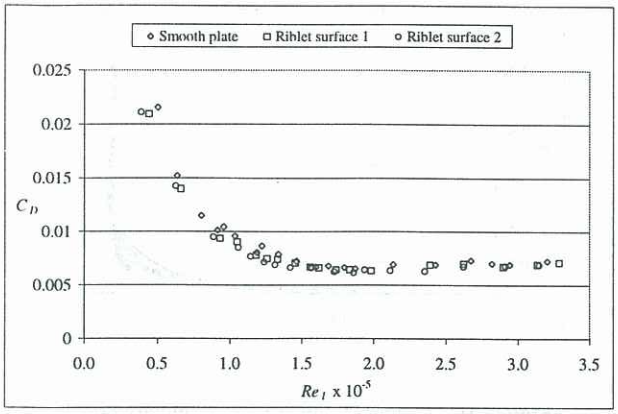


**Figure 7**: Distribution of friction coefficient.

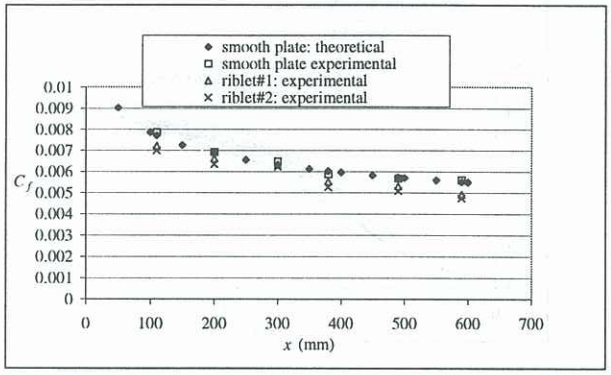


**Figure 8**: Measured drag data for v-groove riblet plates 1 and 2.